Structure and internal rotation in the S_0 and S_1 states of *o*-toluidine studied by high resolution UV spectroscopy

Ivo Kalkman,[a] Chau Vu,[b] Michael Schmitt*[b] and W. Leo Meerts*[a]

Received 26th November 2008, Accepted 23rd February 2009
First published as an Advance Article on the web 19th March 2009
DOI: 10.1039/b821157d

The rotationally resolved spectrum of the *o*-toluidine $S_1 \leftarrow S_0$ origin was measured using laser induced fluorescence spectroscopy. From the resulting spectrum torsional barriers to internal rotation of the methyl group were derived, which resulted in S_0 state values of $V_3 = 699 \pm 11$ cm^{-1} and $V_6 = 64 \pm 11$ cm^{-1} with an effective rotational constant F of 5.38 ± 0.04 cm^{-1} while for the S_1 state the result was $V_3 = 40.87 \pm 0.14$ cm^{-1} and $V_6 = -16.8 \pm 0.8$ cm^{-1} with $F = 5.086 \pm 0.001$ cm^{-1}. The S_1 state structure was found to be severely distorted, with the methyl group making a 7.7° degree angle with the benzene ring. Evidence of an excited state precessional motion of the methyl group was found.

1. Introduction

One of the fundamental motifs in organic chemistry are aromatic rings, and substituted benzenes have therefore been studied vigorously over the years using a plethora of spectroscopic techniques. Some of the more interesting substitutions involve flexible groups which give rise to dynamics, such as an amino group (aniline) or a methyl group (toluene). In this paper the dynamics in *o*-toluidine (also named *o*-methylaniline), where both these groups are attached to the benzene ring in neighbouring positions, will be investigated.

From aniline it is known that in the ground state its amino group is pyramidal with respect to the benzene plane but that its structure is quasi-planar in the S_1 state.[1,2] From far-infrared (FIR) spectra the inversion barrier was determined to be around 525 cm^{-1}.[3,4] High resolution laser induced fluorescence (LIF) spectra were unable to resolve a tunneling splitting corresponding to the inversion motion, in keeping with this high barrier.[5,6] The situation for the toluidines is very similar. The NH_2 inversion barriers in *o*-, *m*- and *p*-toluidine were measured to be 558, 528 and 588 cm^{-1}, respectively, all a little higher than in aniline due to a higher electron density on the amino nitrogen atom.[7] High-resolution spectroscopy of *p*-toluidine did not reveal a tunneling splitting due to the inversion motion.[8] Such a splitting is therefore not expected to show up in the *o*-toluidine spectrum.

The barrier to internal rotation of the methyl group in substituted toluenes has been investigated for a large number of substituents and substitution positions; a nice overview can be found in a paper by Zhao *et al.*[9] Looking through the tables in this paper a general trend can be observed: for ortho-substituted toluenes electronic excitation dramatically reduces an initially high threefold barrier, whereas for meta-substituted toluenes the methyl group rotation is almost free in the S_0 state but becomes severely hindered in the S_1 state. Since the *para*-substituted toluenes have no threefold barrier due to their higher symmetry their barriers are generally lower, but the same general effect as in *meta*-substituted toluenes can be observed. This means that the barrier height depends much more on the substitution position than on the exact nature of the substituent, and an explanation for these effects is most likely connected to the electronic configuration of these substances. When the substituents considered here, which are all electron donating groups, are replaced with an electron withdrawing group we would therefore expect to see very different behavior, as was confirmed in later experiments on tolunitrile.[10] In the case of *o*-toluidine the barriers to internal rotation were determined from fluorescence excitation and dispersed fluorescence spectra by Okuyama *et al.* which resulted in $V_3 = 703$ cm^{-1}, $V_6 = 62$ cm^{-1} in the S_0 state and $V_3 = 40$ cm^{-1}, $V_6 = -11$ cm^{-1} in the S_1 state.[11] The barrier in the cation was measured to be $V_3 = 649$ cm^{-1}, $V_6 = 19$ cm^{-1}.[12,13]

Calculations on various substituted toluenes have been quite successful in reproducing measured barriers by relating its height to the Hammett σ constant of the substituent combined with substitution position[14] and the difference in π-bond order between both ring carbon bonds geminal to the methyl rotor.[15] These calculations show that the molecular structure changes with rotation of the methyl group, regardless of substituent or substitution position. The molecular geometries and conformational preferences of toluidines are therefore closely connected to the barriers to internal rotation.

p-Toluidine has been studied most extensively since steric hindrance between the methyl and amino groups is absent and it is highly symmetric.[8,16–19] The electronic effects described in the previous paragraph are found to induce a precession of the methyl group with its rotation. Moving to *m*- and *o*-toluidine steric hindrance enhances this precessional motion and leads to distortions of both the methyl and amino groups.[20–23] Simulations by Brodersen *et al.* have revealed that typical changes in rotor axis orientation in substituted toluenes are on the order of 1.5 degrees.[24]

[a] *Molecular- and Biophysics Group, Institute for Molecules and Materials, Radboud University Nijmegen, P.O. Box 9010, NL-6500 GL, Nijmegen, The Netherlands. E-mail: Leo.Meerts@science.ru.nl*
[b] *Heinrich-Heine-Universität, Institut für Physikalische Chemie, D-40225, Düsseldorf, Germany. E-mail: mschmitt@uni-duesseldorf.de*

In this paper the rotational constants of *o*-toluidine in its S_0 and S_1 states will be determined from rotationally resolved UV LIF spectra and these will be used to derive an exact molecular structure. Furthermore, accurate barriers to internal rotation of the methyl group will be derived from the spectra and possible evidence for a precessional motion of the methyl rotor will be discussed.

2. Methods

2.1 Experimental procedures

The experimental setup for the rotationally resolved LIF is described elsewhere.[25] Briefly, it consists of a frequency doubled Nd : YAG laser which pumps a ring dye laser (Coherent 899-21) operated with Rhodamine 6G. The dye laser output is coupled into an external folded ring cavity (Spectra Physics Wavetrain) for second harmonic generation. The typical output power is 20 mW and is constant during each experiment.

The molecular beam is formed by co-expanding argon at a backing pressure of 340 mbar and room temperature *o*-toluidine into the vacuum through a 320 μm nozzle. The molecular beam machine consists of three differentially pumped vacuum chambers that are linearly connected by skimmers (1 mm and 3 mm diameter, respectively). In the third chamber, 360 mm downstream of the nozzle, the UV laser beam crosses the molecular beam at right angles. Imaging optics focus the total undispersed fluorescence from the excited molecules onto a photo-multiplier tube mounted perpendicular to the plane defined by the laser and the molecular beam. Its output is discriminated and digitized by a photon counter card inside a personal computer. The Doppler width of measured transitions is 25 MHz (FWHM). Relative frequencies are determined with a quasi-confocal Fabry-Perot interferometer with a free spectral range (FSR) of 149.9434(56) MHz. The absolute frequency is obtained by comparing the recorded iodine absorption spectrum with tabulated lines.[26]

o-Toluidine ($\geq 99\%$) was obtained from Aldrich and used without further purification.

2.2 Computational methods

2.2.1 ***Ab initio*** **calculations.** Structure optimizations were performed employing the valence triple zeta basis set with polarization functions (d,p) from the TURBOMOLE library.[27,28] The equilibrium geometries of the electronic ground and the lowest excited singlet states were optimized at the CC2 level within the resolution-of-the-identity approximation.[29,30] Ground state vibrational frequencies have been calculated through analytical second derivatives using the AOFORCE module[31,32] implemented in Turbomole Version 5.8. Excited state vibrational frequencies were calculated using numerical differentiation of analytic gradients using the NumForce script of Turbomole Version 5.8.

The singlet state energies, wavefunctions, and transition dipole moments were calculated using the combined density functional theory/multi-reference configuration interaction (DFT/MRCI) method by Grimme and Waletzke.[33] The configuration state functions (CSFs) in the MRCI expansion are constructed from Kohn–Sham (KS) orbitals, optimized for the dominant closed shell determinant of the electronic ground state employing the BH-LYP functional.[34,35] All valence electrons were correlated in the MRCI runs and the eigenvalues and eigenvectors of the lowest singlet state were determined. The initial set of reference configuration state functions was generated automatically in a complete active space type procedure (including all single and double excitations from the five highest occupied molecular orbitals in the KS determinant to the five lowest virtual orbitals) and was then iteratively improved. The MRCI expansion was kept moderate by extensive configuration selection. The selection of the most important CSFs is based on an energy gap criterion as described by Grimme and Waletzke.[33] Only those configurations were taken into account whose energy did not exceed a certain cutoff energy. The energy of a given configuration was estimated from orbital energies within the selection procedure. The cutoff energy was given by the energy of the highest desired root as calculated for the reference space plus a cutoff parameter $\delta E_{\mathrm{sel}} = 1.0 E_H$. This choice has been shown to yield nearly converged results.[33]

2.2.2 Spectral analysis. To describe the *o*-toluidine spectrum a torsion–rotation Hamiltonian of the following form was used:[36]

$$H_{\mathrm{tr}} = F(p - \vec{\rho}\vec{J})^2 + V(\alpha) + AJ_a^2 + BJ_b^2 + CJ_c^2. \qquad (1)$$

In this equation A, B and C are the molecule's rotational constants, J_a, J_b and J_c are the projections of the total angular momentum $\vec{J}$ onto the main inertial axes a, b and c, respectively, and $V(\alpha)$ is the torsional potential, which takes the form:

$$V(\alpha) = \frac{V_3}{2}(1 - \cos 3\alpha) + \frac{V_6}{2}(1 - \cos 6\alpha). \qquad (2)$$

Furthermore, $p = -i\hbar\frac{\partial}{\partial\alpha}$ is the angular momentum operator conjugate to the torsional angle α and F is the internal rotation constant, which is related to the moment of inertia of the internal rotor I_α and its torsional constant, F_{top}, *via*:

$$F = \hbar^2/2rI_\alpha = F_{\mathrm{top}}/r, \qquad (3)$$

with

$$r = 1 - I_\alpha \sum_g \cos^2(\eta_g)/I_g. \qquad (4)$$

I_g ($g = a,b,c$) are the moments of inertia of the entire molecule and cos η_g are the direction cosines of the methyl top axis with respect to the main inertial axes. Finally, the parameter ρ in eqn (1) is related to these direction cosines through the equation:

$$\rho_g = (I_\alpha/I_g)\cos\,\eta_g. \qquad (5)$$

This equation can be rewritten in terms of the polar angles (ζ,η), where ζ is the angle between the methyl top axis and the c-axis and η is the angle between the projection of the methyl top axis onto the ab-plane and the a-axis. When this is done the components of ρ are given by:

$$\begin{aligned} \rho_a &= (I_\alpha/I_a)\sin\,\zeta\,\cos\,\eta \\ \rho_b &= (I_\alpha/I_b)\sin\,\zeta\,\sin\,\eta \\ \rho_c &= (I_\alpha/I_c)\cos\,\zeta. \end{aligned} \qquad (6)$$

It will be shown in section 3 that the torsional splitting in the ground state is too small to be measured in the experiment described here, which means that no information on the corresponding ground state parameters can be derived. The only information on the torsional potential that can be extracted from the spectrum are the values of V'_3, F', η' and ζ'. An initial fit of the rotationally resolved spectrum was performed with the Evolutionary Algorithm (EA) automatic fitting program[37–39] using the recently implemented DR2 algorithm.[40] For this fit the values of V''_3, V''_6, F'' and V'_6 were taken from Okuyama *et al.*[11] while the values for η'' and ζ'' were fixed to those that resulted from RICC2 calculations. In a second step the resulting V'_3, F', η' and ζ' were used in combination with torsional transition frequencies measured by laser induced fluorescence[23] and dispersed fluorescence[11] spectroscopy to determine the values of the torsional parameters that were kept fixed in the first fit. This was done with the program HTorFit.[41]

3. Results and discussion

Fig. 1 shows the rotationally resolved S1 ← S_0 origin spectrum of *o*-toluidine. It consists of two spectral components separated by 98 584 ± 5 MHz. As has been shown previously[22,23] these result from transitions between the two lowest torsional levels which arise from internal rotation of the methyl group. The lower of the two components is due to transitions between nondegenerate levels of a_1 symmetry while the upper one results from transitions between doubly degenerate torsional levels of *e* symmetry. Shown in the panel below the spectrum is the best fit. The correspondence between the two is excellent, as is also evidenced by the enlarged portion depicted in the two panels below it. The bottom panel of Fig. 1 shows a stick spectrum of the strongest transitions in the simulation and a convolution of these with a Lorentzian function with a width (FWHM) of 0.3 cm^{-1}; the resulting spectrum matches the rotational contour spectra from Ballesteros and Santos[23] quite well.

From the ordering of the two torsional components it can immediately be concluded that the barrier to internal rotation must be lower in the S_1 state than it is in the S_0 state. To obtain exact values for the barriers to internal rotation a combined fit of this spectrum with the torsional bands measured in previous work[11,23] was performed as described in section 2.2.2. The molecular parameters deduced from this analysis, together with the values obtained from *ab initio* calculations, are given in Table 1. Calculated torsional transitions are compared with measured ones in Table 2. From the second table it can be seen that, again, the deduced parameters are in excellent agreement with experiment.

A two-temperature model[42] was used to describe the rotational temperature in the molecular beam, which yielded T_1 = 2.1 K and T_2 = 3.6 K with a relative T_2 weight of 0.14. From a 26.8 MHz Lorentzian contribution to the total linewidth the excited state lifetime is found to be around 6.0 ns, which is substantially longer than the 3.5 ns lifetime in *p*-toluidine[8] and much closer to the 7.2 ns measured in aniline.[2]

3.1 Transition dipole moment

The value of ϕ in Table 1 indicates that the transition dipole moment (TDM) lies in the plane of the benzene ring. While the sign of the angle θ normally cannot be determined from the experiment since the relative intensities in the spectrum only depend on the square of the transition dipole moment components, its sign can be determined in molecules that possess an internal rotor. This happens because the intensities of some of the *E*-type transitions depend on the relative signs of θ and η.[43–45] Since the sign of η is known from geometrical considerations this fixes the absolute sign of θ. In the case at hand the result is that the TDM orientation has to be in the direction of the methyl group, which corresponds to the plus sign in Fig. 2.

From a comparison of the measured rotational constants with those resulting from RICC2 calculations it can be seen that the correspondence is satisfactory, and as will be discussed in section 3.3 the calculations indicate that the amino group is nonplanar in the S_0 state and becomes more planar in the S_1 state. This effect is also observed in aniline, where the transition dipole moment is perpendicular to the amino group CN bond.[2,46] Because the methyl group has a relatively small influence on the benzene π-electron system compared to the amino group (inductive *vs.* mesomeric effect) it therefore seems reasonable to conclude that the electronic excitation must be similar to that in aniline and the transition dipole moment is directed towards the methyl group, which only induces a moderate change in the TDM direction with respect to that in aniline.

As can be seen from Table 1, the RICC2 calculations also predict the torsional barriers very accurately. Since the torsional barrier in *o*-toluidine is very sensitive to the local electronic environment at the ring carbon atom the methyl group is attached to, this is another indication that the *ab initio* results are reliable. However, Table 1 shows that it doesn't predict the S_1 ← S_0 excitation energy very accurately. Moreover, no information on the sign of the θ angle can be extracted from it. A single point DFT/MRCI calculation at the RICC2 optimized S_1 state geometry was therefore performed, the results of which were added to Table 1. Both the size and the direction of the resulting TDM as well as the excitation energy agree very well with experiment.

3.2 The methyl rotor

The last piece of information that results from the spectral analysis concerns the methyl rotor geometry contained in the parameters F, η and ζ. To avoid confusion both the values for F and F_{top} defined in eqn (3) are given in Table 1. Immediately apparent is the fact that the parameter ζ has a value which is very different from 90° in the S_1 state. This is certainly not expected and the possibility that the rotor actually makes an 18.4° angle with respect to the *ab*-plane is ruled out by the inertial defect, which points to an almost planar structure. This interpretation is therefore disregarded, and since a reasonable correspondence between model and experiment could only be obtained with the parameter values given in Table 1 it seems that an alternate model is needed.

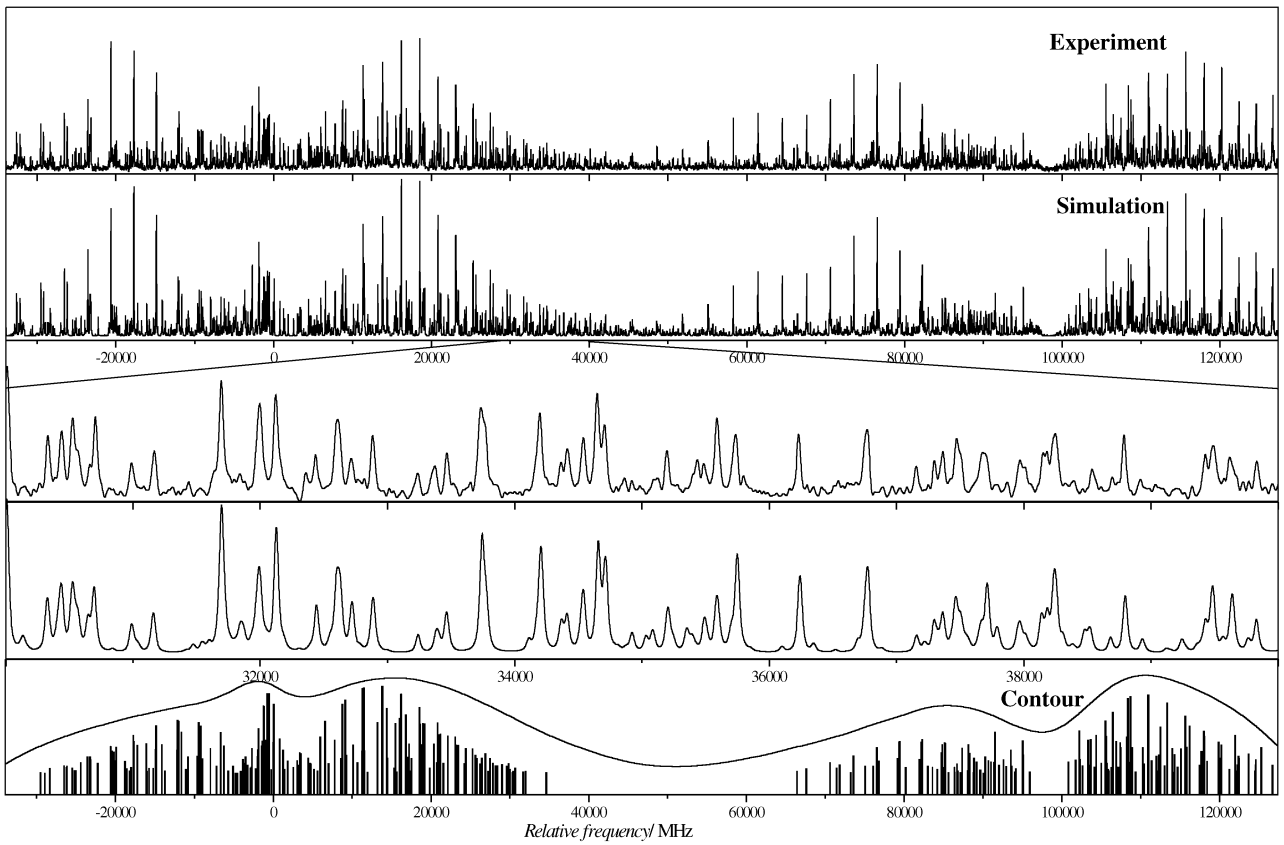

Fig. 1 The electronic origin of *o*-toluidine at 34 316.848 cm^{-1}. The upper two traces show the measured spectrum and the best simulation. In the two traces below that an enlarged part of the spectrum is shown. The bottom trace shows a stick spectrum which contains the strongest transitions from the simulation shown in the second trace and a convolution of these with a Lorentz function (FWHM 0.3 cm^{-1}).

Table 1 Molecular parameters of *o*-toluidine as determined from the fits to the $S_1 \leftarrow S_0$ origin transition shown in Fig. 1. For a description of the fitting procedure see section 2.2.2. Also listed are the results of *ab initio* calculations at the RICC2/TZVP and DFT/MRCI levels of theory

	S_0			S_1				$\Delta(S_1 - S_0)$
	Exp.	RICC2	Ref. 11	Exp.	RICC2	Ref. 11	Ref. 21	Exp.
A/MHz	3229.60(17)	3268	—	3121.92(14)	3098	—	—	—107.68(18)
B/MHz	2188.49(16)	2219	—	2181.97(13)	2187	—	—	−6.52(22)
C/MHz	1316.82(9)	1334	—	1296.03(12)	1295	—	—	−20.79(13)
ΔI/amu Å^2	−3.62(4)	−3.59	—	−3.60(5)	−4.00	—	—	0.02(5)
V_3/cm^{-1}	699(11)	657	703	40.87(14)	120	40	35	−658(11)
V_6 (cm^{-1})	64(11)	—	62	−16.8(8)	—	−11	28	−81(11)
F_{top}/cm^{-1}	5.28(4)	5.51	5.18	5.086(1)	5.48	5.30	5.1	−0.19(4)
F/cm^{-1}	5.38(4)	5.62	5.28	5.184(1)	5.59	5.40	5.2	−0.19(4)
η/°	28.7[a]	28.7	—	28.14(12)	26.1	—	—	7.1(23)
ζ/°	89.5[a]	89.5	—	71.6(7)	88.1	—	—	−18.3(6)

	Exp.	RICC2	DFT/MRCI	Ref. 11	Ref. 21
θ/°	+37.47(26)	±31.5	+38.9	—	—
ϕ/°	89.3(8)	90.0	88.9	—	—
ν_0/cm^{-1}	34 316.848(1)	36 137	34 706	34 316	34 316
$\nu_0(E)$–$\nu_0(A_1)$/MHz	98 584(5)	—	—	≈90 000	≈105 000
$\Delta_{Lorentz}$/MHz	26.8(10)	—	—	—	—
$\tau_{1/2}$/ns	5.95(22)	—	—	—	—

[a] Fixed to RICC2 calculated value.

For the interpretation of *p*-toluidine spectra Tan *et al.*[8] were forced to use a modified Hamiltonian which accounts for a precessional motion of the methyl rotor axis. Although in the case considered here a fit to the data is possible without inclusion of a precession angle it cannot be ruled out that a second, physically more acceptable solution is possible when it is included. The appropriate form of this Hamiltonian, including a V_3 potential term, was therefore used in an attempt to obtain

Table 2 Torsional transitions used in the determination of some of the internal rotor parameters of *o*-toluidine given in Table 1. For a description of the fitting procedure see section 2.2.2. All values are relative to the $0a_1 \leftarrow 0a_1$ transition, where $\nu\sigma(S_1) \leftarrow \nu\sigma(S_0)$ indicates an absorption band and $\nu\sigma(S_1) \rightarrow \nu\sigma(S_0)$ an emission band

Transition	Exp.	Fit	Diff.	
$1e \leftarrow 1e$	98584(5)[a]	98 584	0	MHz
$1e \leftarrow 2e$	27.8(3)[b]	27.4	−0.4	cm^{-1}
$0a_1 \leftarrow 3a_2$	45.0(3)[b]	45.5	+0.5	cm^{-1}
$0a_1 \leftarrow 3a_1$	56.2(3)[b]	57.5	+1.3	cm^{-1}
$1e \leftarrow 4e$	86.8(3)[b]	87.8	+1.0	cm^{-1}
$1e \leftarrow 5e$	132.1(3)[b]	134.0	+1.9	cm^{-1}
$0a_1 \leftarrow 6a_1$	196.6(3)[b]	190.9	−5.7	cm^{-1}
$1e \rightarrow 2e$	182(6)[c]	189	+7	cm^{-1}
$0a_1 \rightarrow 3a_1$	361(6)[c]	358	−3	cm^{-1}
$1e \rightarrow 4e$	362(6)[c]	355	−7	cm^{-1}
$1e \rightarrow 5e$	472(10)[c]	489	+17	cm^{-1}
$0a_1 \rightarrow 6a_1$	578(10)[c]	578	0	cm^{-1}
$1e \rightarrow 7e$	589(10)[c]	602	+13	cm^{-1}
$1e \rightarrow 8e$	684(10)[c]	669	−15	cm^{-1}

[a] This work. [b] Ballesteros and Santos.[23] [c] Okuyama *et al.*[11]

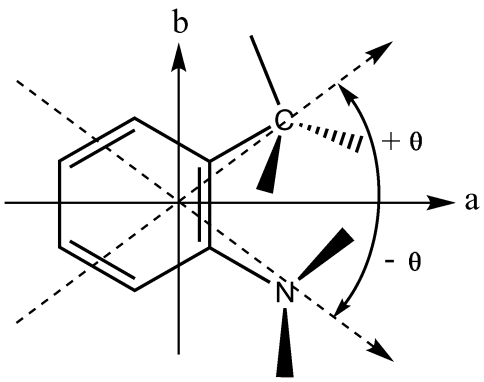

Fig. 2 Definition of the transition dipole moment direction with respect to the main interial axes.

a fit, but this resulted in a zero degree precession angle. However, this does not rule out the possibility that precessional motion is responsible for the observed effective value of ζ. As was pointed out by Brodersen and Gordon[24] this Hamiltonian does not allow for any motion of the methyl carbon atom with the torsional angle and it is therefore still possible that the observed effect is due to motion of the *whole* methyl group. They showed that this results in a marked decrease of the effective rotational constant F with respect to its equilibrium value, and that a precession angle of 1.5° is typical of substituted toluenes. Looking at Table 1, indeed it can again be seen that the measured values are much smaller than the calculated ones and that the difference between the two is much larger in the S_1 state than it is in S_0. The fact that the *ab initio* results predict that the angle ζ becomes 88.1° on electronic excitation, which would mean that the methyl group comes out of the plane by 1.9°, can be viewed as further evidence to support this theory. For this situation the Hamiltonian used in the present analysis (given in eqn (1)) is only approximate and, as a result, the value of ζ found here should not be viewed as a geometric parameter but rather as an effective parameter which includes perturbation effects.

3.3 Molecular structure

As was already noted in section 3.1 the rotational constants that result from RICC2 calculations compare favourably with those obtained from the experiment, which adds credibility to the structure derived from them. A list of geometric parameters is given in Table 3; the corresponding atomic numbering is depicted in Fig. 3.

For the S_0 state it can be seen that, with the exception of the C_8H_{8a} bond, all bond lengths are shorter than in either of the two calculations performed so far. In the S_1 state the opposite is found, and most bond lengths tend to be longer. In combination with the observation that almost all bond lengths increase on electronic excitation, this means that the effect the excitation has on the *o*-toluidine geometry is much greater than previously thought. This picture is confirmed by the bond angles: whereas in the ground state they coincide very well with the values from previous work, they differ substantially in the electronically excited state.

When the detailed benzene ring geometry is investigated it can be seen that in the S_0 state the ring carbon bond between both atoms the substituents attach to, C_1C_2, is longest whereas the one on the opposite side of the ring, C_4C_5, is shortest. Furthermore, the $C_1C_2C_3$ angle is only 118.5° whereas the $C_2C_3C_4$ angle is 122.0°. These all act to tilt the methyl group away from the amino group. Since the amino group is electron withdrawing in nature, an attempt to explain this using only natural hybrid orbitals (NHOs), as was done for *o*-chlorotoluene and *o*-fluorotoluene by Lu *et al.*,[15] would lead us to expect that the $C_6C_1C_2$ angle is substantially larger than 120°. This is not the case, with its actual value at 119.6° even slightly smaller than 120°. Moreover, NHOs have a local effect on the ring structure and cannot explain the fact that the C_4C_5 bond is shorter than both its neighbours. These results are therefore viewed as evidence that, unlike in *o*-chlorotoluene and *o*-fluorotoluene, steric hindrance is an important factor for the *o*-toluidine structure.

The approximate C_2 symmetry axis (from an inertial point of view) which the benzene ring possesses in the ground state, intersecting both the C_1C_2 and the C_4C_5 bonds, is retained on electronic excitation. Simultaneously, all ring CC bond lengths increase, which corresponds to an expansion of the ring. With respect to the average ring CC distance, the C_2C_3 and C_6C_1 bonds are elongated while the C_2C_3 and C_5C_6 bonds are shortened. Combined with the fact that both the C_2C_8 and the C_1N_7 bonds lengths increase, this means that the S_1 state is strongly *ortho*-quinoidal in character. From the ring dihedral angles it can be deduced that the ring geometry also becomes distorted in the out-of-plane direction and adopts a chair conformation similar to that of cyclohexane. Interestingly, while the difference between both CC bond lengths geminal to the methyl group (C_1C_2 and C_2C_3) is 0.3 pm smaller in the excited state than it is in the ground state, they are by no means equal. This means that the barrier to internal rotation of the methyl group is low in the S_1 state even though good, local C_{2v} symmetry at the C_2 carbon atom is absent. This confirms the conclusion from earlier work that the barrier is mostly electronic in nature and that steric effects are only of secondary importance.[14,15]

Table 3 Rotational constants and S_0 and S_1 state geometric parameters for *o*-toluidine. The calculated values from this work were obtained at the RICC2/TZVP level of theory. The atomic numbering refers to Fig. 3

	S_0				S_1		
	Exp.[a]	RICC2[a]	MP2[b]	HF[c]	Exp.[a]	RICC2[a]	CIS[b]
A/MHz	3229.60	3268	3228	—	3121.92	3098	3196
B/MHz	2188.49	2219	2178	—	2181.97	2187	2240
C/MHz	1316.82	1334	1313	—	1296.03	1295	1328
Bond lengths/pm							
C_1C_2	—	139.8	141.1	140.1	—	142.9	142.7
C_2C_3	—	138.3	140.0	138.8	—	144.1	137.0
C_3C_4	—	138.4	139.8	138.8	—	141.9	140.0
C_4C_5	—	138.0	139.8	138.5	—	141.6	139.8
C_5C_6	—	138.1	139.6	138.5	—	142.2	136.3
C_6C_1	—	138.7	140.3	139.2	—	143.5	143.6
C_1N_7	—	139.9	141.0	140.1	—	137.2	131.1
C_2C_8	—	150.8	150.5	151.1	—	149.4	150.1
CH (ring)[d]	—	107.5	108.9	107.6	—	108.4	107.3
N_7H_{7a}	—	99.5	101.7[d]	99.8[d]	—	101.1	100.4[d]
N_7H_{7b}	—	99.5	101.7[d]	99.8[d]	—	101.1	100.4[d]
C_8H_{8a}	—	108.8	109.6[d]	108.6[d]	—	109.9	108.4[d]
C_8H_{8b}	—	108.5	109.6[d]	108.6[d]	—	109.3	108.4[d]
C_8H_{8c}	—	108.2	109.6[d]	108.6[d]	—	109.4	108.4[d]
C_1C_4	—	278.4	281.0	279.3	—	281.3	278.8
Bond angles/°							
$C_1C_2C_3$	—	118.5	118.6	118.5	—	116.7	117.4
$C_2C_3C_4$	—	122.0	121.6	122.0	—	119.0	121.9
$C_3C_4C_5$	—	118.9	119.2	118.9	—	122.4	121.0
$C_4C_5C_6$	—	120.1	120.0	120.1	—	119.4	119.5
$C_5C_6C_1$	—	120.8	120.7	120.8	—	117.9	120.4
$C_6C_1C_2$	—	119.6	119.7	119.6	—	123.2	119.9
$N_7C_1C_2$	—	120.3	119.7	120.2	—	119.5	121.3
$N_7C_1C_6$	—	120.1	120.6	120.1	—	116.8	118.8
$C_1C_2C_8$	—	120.6	120.0	120.6	—	123.2	121.1
$C_3C_2C_8$	—	120.9	121.4	120.9	—	119.8	121.5
$H_{7a}N_7C_1$	—	115.1	114.2	—	—	119.0	123.1
$H_{7b}N_7C_1$	—	114.1	113.2	—	—	117.5	121.2
$H_{7a}N_7H_{7b}$	—	111.0	109.9	110.1	—	116.1	115.7
$C_2C_8H_{8a}$	—	111.8	—	111.3[d]	—	112.4	—
$C_2C_8H_{8b}$	—	111.3	—	111.3[d]	—	113.1	—
$C_2C_8H_{8c}$	—	110.7	—	111.3[d]	—	109.7	—
$H_{8a}C_8H_{8b}$	—	107.5	107.3[d]	107.5[d]	—	107.9	108.0[d]
$H_{8b}C_8H_{8c}$	—	108.0	107.3[d]	107.5[d]	—	106.7	108.0[d]
$H_{8c}C_8H_{8a}$	—	107.3	107.3[d]	107.5[d]	—	106.6	108.0[d]
Dihedral angles/°							
$C_1C_2C_3C_4$	—	−0.5	—	—	—	−6.0	—
$C_2C_3C_4C5$	—	−0.1	—	—	—	1.9	—
$C_3C_4C_5C_6$	—	0.2	—	—	—	−4.4	—
$C_4C_5C_6C_1$	—	0.2	—	—	—	10.4	—
$C_5C_6C_1C_2$	—	−0.7	—	—	—	−13.6	—
$C_6C_1C_2C_3$	—	0.9	—	—	—	11.8	—
$C_5C_6C_1N_7$	—	−177.3	−176.8	—	—	−177.5	0.0
$C_6C_1N_7H_{7a}$	—	−148.5	—	—	—	−165.5	—
$C_6C_1N_7H_{7b}$	—	−18.5	—	—	—	−16.8	—
$C_4C_3C_2C_8$	—	179.2	—	—	—	172.3	—
$C_3C_2C_8H_{8a}$	—	116.0	—	—	—	79.0	—
$C_3C_2C_8H_{8b}$	—	−123.7	—	—	—	−158.5	—
$C_3C_2C_8H_{8c}$	—	−3.6	—	—	—	−39.4	—

[a] This work. [b] MP2/6-31+G* (S_0) and CIS/6-31+G* (S_1), Ballesteros and Santos.[23] [c] HF/6-31+G*, Tzeng *et al.*[22] [d] Average value.

From the geometries of the methyl and amino groups it is deduced that steric hindrance not only affects the benzene ring, but also both substituents themselves. In the ground state it can be seen from the methyl group dihedral angles that it is rotated by about 3.8° with respect to its equilibrium position in toluene, which has the C_8H_{8c} bond in the plane of the benzene ring. For the amino group the combination of steric repulsion and the addition of another electron donating group to the ring causes it to be much more planar than in aniline (where it is out of plane by a 37.5° angle[2]) and tilted away from the methyl rotor, with one hydrogen atom 31.5° below the plane and the other just 18.5°. In the electronically excited state the amino group becomes more planar due to sharing its lone pair electron with the benzene π-electron system, which points to electronic excitation comparable to that in aniline. As a result, the methyl group orientation is now completely different, with the C_8H_{8a} bond in a much more vertical position, not unlike the situation in toluene.[47] Especially for the methyl group the

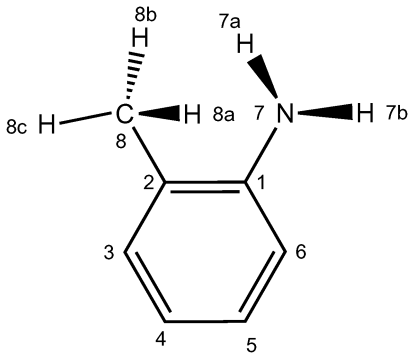

Fig. 3 Atomic numbering of *o*-toluidine used in Table 3.

distortions in the S_1 state are severe, with the three C_2C_8H bond angles differing by as much as 3.4°. Most significantly though, from the $C_4C_3C_2C_8$ dihedral angle the methyl carbon atom is found to move out of the plane of the benzene ring by as much as 7.7°. This supports the explanation that the effective value of 71.6° found for ζ in section 3.2 is due to a precessional motion of the whole methyl group.

4. Conclusions

The $S_1 \leftarrow S_0$ transition in *o*-toluidine has been measured using rotationally resolved electronic spectroscopy. The resulting spectrum consists of two overlapping spectral components which can be assigned to the $0a_1 \leftarrow 0a_1$ and $1e \leftarrow 1e$ transitions between torsional sub-bands that arise from internal rotation of the methyl group. The torsional parameters that can be derived were combined with frequencies of torsional transitions from previous work[11,23] to derive accurate barriers to internal rotation in both electronic states. It was found that the V_3 barrier is lowered from 699 cm^{-1} in the S_0 state to 40.87 cm^{-1} in the S_1 state. This dramatic lowering of the barrier to internal rotation is similar to that observed in other *ortho*-substituted toluenes[9] and can be explained in terms of the difference in π-bond order between both ring carbon bonds geminal to the methyl rotor.[15]

The rotational constants that were determined for both electronic states are close to those resulting from RICC2 calcultions, and an extensive analysis of the predicted molecular geometry was therefore made. As is usual for substituted benzenes, the benzene ring was found to expand on electronic excitation, and the amino group becomes more planar. The excited state geometry has a strongly *ortho*-quinoidal character which shortens both the methyl CC bond and the amino CN bond. *Para*-quinoidal distortion is frequently encountered in *p*-substituted benzenes on electronic excitation[48–50] and given the fact that *o*- and *p*-substituted benzenes are electronically similar this is therefore not unexpected. As a result, the steric interactions between both substituents, which are already visible in the S_0 state, are increased dramatically in the S_1 state: the methyl group makes a 7.7° angle with the local benzene ring orientation and rotates away from the S_0 state geometry. Combined with the fact that an unrealistically large angle between the normal of the benzene plane and the methyl rotor axis resulted from spectral analysis and that the effective rotational constant *F* was found to decrease dramatically on electronic excitation, this constitutes a compelling evidence for an S_1 state precessional motion of the whole methyl group.[24]

Acknowledgements

This work has been performed in the SFB 663 TP A2, Universität Düsseldorf and was printed upon its demand with financial support from the Deutsche Forschungsgemeinschaft. The authors like to thank the National Computer Facilities of the Netherlands Organisation for Scientific Research (NWO) for a grant on the Dutch supercomputing facility SARA. This work was also supported by the Netherlands Organization for Scientific Research and the Deutsche Forschungsgemeinschaft in the framework of the NWO-DFG bilateral programme (SCHM1043/10-1).

References

1 N. Mikami, A. Hiraya, I. Fujiwara and M. Ito, *Chem. Phys. Lett.*, 1980, **74**, 531–535.
2 W. E. Sinclair and D. W. Pratt, *J. Chem. Phys.*, 1996, **105**, 7942.
3 N. W. Larsen, E. L. Hansen and F. M. Nicolaisen, *Chem. Phys. Lett.*, 1976, **43**, 584–586.
4 R. A. Kydd and P. J. Krueger, *Chem. Phys. Lett.*, 1977, **49**, 539–543.
5 E. R. T. Kerstel, M. Becucci, G. Pietraperzia and E. Castellucci, *Chem. Phys.*, 1995, **199**, 263–273.
6 E. R. T. Kerstel, M. Becucci, G. Pietraperzia, D. Consalvo and E. Castellucci, *J. Mol. Spectrosc.*, 1996, **177**, 74–78.
7 R. A. Kydd and P. J. Krueger, *J. Chem. Phys.*, 1980, **72**, 280–283.
8 X.-Q. Tan and D. W. Pratt, *J. Chem. Phys.*, 1994, **100**, 7061.
9 Z.-Q. Zhao, C. S. Parmenter, D. B. Moss, A. J. Bradley, A. E. W. Knight and K. G. Owens, *J. Chem. Phys.*, 1992, **96**, 6362–6377.
10 M. Fujii, M. Yamauchi, K. Takazawa and M. Ito, *Spectrochim. Acta, Part A*, 1994, **50**, 1421–1433.
11 K. Okuyama, N. Mikami and M. Ito, *Laser Chem.*, 1987, **7**, 197.
12 H. Ikoma, K. Takazawa, Y. Emura, S. Ikeda, H. Abe, H. Hayashi and M. asaaki Fujii, *J. Chem. Phys.*, 1996, **105**, 10201–10209.
13 J. L. Lin, K. C. Lin and W. B. Tzeng, *J. Phys. Chem. A*, 2002, **106**, 6462–6468.
14 H. Nakai and M. Kawai, *J. Chem. Phys.*, 2000, **113**, 2168–2174.
15 K. T. Lu, F. Weinhold and J. C. Weisshaar, *J. Chem. Phys.*, 1995, **102**, 6787.
16 D. E. Powers, J. B. Hopkins and R. E. Smalley, *J. Chem. Phys.*, 1980, **72**, 5721–5730.
17 R. Tembreull, T. M. Dunn and D. M. Lubman, *Spectrochim. Acta, Part A*, 1986, **42**, 899.
18 W. B. Tzeng and K. Narayanan, *J. Mol. Struct.*, 1998, **446**, 93–102.
19 S. Yan and L. H. Spangler, *J. Chem. Phys.*, 1992, **96**, 4106–4117.
20 L. Santos, E. Martínez, B. Ballesteros and J. Sanchez, *Spectrochim. Acta, Part A*, 2000, **56**, 1905–1915.
21 R. Disselkamp, H. S. Im and E. R. Bernstein, *J. Chem. Phys.*, 1992, **97**, 7889–7901.
22 W. B. Tzeng, K. Narayanan, J. L. Lin and C. C. Tung, *Spectrochim. Acta, Part A*, 1999, **55**, 153.
23 B. Ballesteros and L. Santos, *Spectrochim. Acta, Part A*, 2002, **58**, 1069–1081.
24 P. M. Brodersen and R. D. Gordon, *J. Mol. Struct.*, 2000, **522**, 279–288.
25 M. Schmitt, J. Küpper, D. Spangenberg and A. Westphal, *Chem. Phys.*, 2000, **254**, 349–361.
26 S. Gerstenkorn and P. Luc, *Atlas du spectre d'absorption de la molécule d'iode*, CNRS, Paris, 1982.
27 R. Ahlrichs, M. Bär, M. Häser, H. Horn and C. Kölmel, *Chem. Phys. Lett.*, 1989, **162**, 165–169.
28 A. Schäfer, C. Huber and R. Ahlrichs, *J. Chem. Phys.*, 1994, **100**, 5829–5835.
29 C. Hättig and A. Köhn, *J. Chem. Phys.*, 2002, **113**, 6939.
30 C. Hättig, *J. Chem. Phys.*, 2002, **117**, 7751–7761.

31 H. Horn, H. Weiss, M. Häser, M. Ehrig and R. Ahlrichs, *J. Comput. Chem.*, 1991, **12**, 1058.
32 P. Deglmann, F. Furche and R. Ahlrichs, *Chem. Phys. Lett.*, 2002, **362**, 511–518.
33 S. Grimme and M. Waletzke, *J. Chem. Phys.*, 1999, **111**, 5645–5655.
34 A. D. Becke, *J. Chem. Phys.*, 1993, **98**, 1372.
35 C. Lee, W. Yang and R. Parr, *Phys. Rev. B*, 1988, **37**, 785–789.
36 W. Gordy and R. L. Cook, *Microwave Molecular Spectra*, Wiley, New York, 3 edn, 1984.
37 J. A. Hageman, R. Wehrens, R. de Gelder, W. L. Meerts and L. M. C. Buydens, *J. Chem. Phys.*, 2000, **113**, 7955–7962.
38 W. L. Meerts, M. Schmitt and G. Groenenboom, *Can. J. Chem.*, 2004, **82**, 804–819.
39 W. L. Meerts and M. Schmitt, *Int. Rev. Phys. Chem.*, 2006, **25**, 353–406.
40 I. Kalkman, C. Vu, M. Schmitt and W. L. Meerts, *ChemPhysChem*, 2008, **9**, 1788–1797.
41 C. Jacoby, M. Böhm, C. Vu, C. Ratzer and M. Schmitt, *ChemPhysChem*, 2006, **7**, 448–455.
42 Y. R. Wu and D. H. Levy, *J. Chem. Phys.*, 1989, **91**, 5278–5284.
43 D. F. Plusquellic and D. W. Pratt, *J. Chem. Phys.*, 1992, **97**, 8970.
44 K. Remmers, E. Jalviste, I. Mistrík, G. Berden and W. L. Meerts, *J. Chem. Phys.*, 1998, **108**, 8436–8445.
45 G. Myszkiewicz, W. L. Meerts, C. Ratzer and M. Schmitt, *Phys. Chem. Chem. Phys.*, 2005, **7**, 2142–2150.
46 T. M. Korter, D. R. Borst, C. J. Butler and D. W. Pratt, *J. Am. Chem. Soc.*, 2001, **123**, 96–99.
47 D. R. Borst and D. W. Pratt, *J. Chem. Phys.*, 2000, **113**, 3658–3669.
48 M. Böhm, C. Ratzer and M. Schmitt, *J. Mol. Struct.*, 2005, **800**, 55–61.
49 M. Schmitt, C. Ratzer, C. Jacoby and W. L. Meerts, *J. Mol. Struct.*, 2005, **742**, 123–130.
50 J. W. Ribblett, D. R. Borst and D. W. Pratt, *J. Chem. Phys.*, 1999, **111**, 8454–8461.

